Dynamics and Mechanisms of
Photoinduced Transfer and Related Phenomena
N. Mataga, T. Okada and H. Masuhara (Editors)

SOLVATION DYNAMICS IN ELECTRON-TRANSFER AND FEMTOSECOND NONLINEAR SPECTROSCOPY

Shaul Mukamel and Wayne Bosma

Department of Chemistry, University of Rochester, Rochester, NY 14627

Abstract

A unified theory for electron-transfer rate and hole-burning spectroscopy is presented using the density matrix and its evolution in Liouville space. Both solvent modes and high frequency intramolecular modes are incorporated in the same manner using a multimode Brownian oscillator model for the nonlinear response function.

I. Introduction

Solvent-solute interactions play an important role in chemical processes and optical spectroscopy in condensed-phases. Laser pulses with durations as short as ~ 10 fs may be used in nonlinear optical experiments to probe the solute and solvent degrees of freedom separately.[1-2] Additionally, a solvated molecule's interaction with its solvent environment directly affects the rates of electron-transfer processes.[3-6]

We have developed a microscopic theory based on the evolution of the density matrix, which establishes a general fundamental connection between electron-transfer rates and nonlinear optical processes in solution.[8] Solvent correlation functions and dephasing rates obtained from nonlinear optical measurements may thus be directly used in the calculation of molecular rate processes. This theory provides an insight on the transition from nonadiabatic to adiabatic rates, and the relevant solvent timescale which controls the adiabaticity is precisely defined. In addition, the incorporation of internal vibrational modes of the solute can be made in the current theory in a straightforward way. We shall discuss here the application of this density-matrix approach to a multimode solute-solvent system, where we consider specifically the vibronic states of one or more solute modes. We shall present a semiclassical theory which provides a unified description of molecular rate processes and nonlinear optical lineshapes. We

will furthermore develop in parallel formulas for the electron-transfer rate and the ultrafast hole-burning signal, to reveal the exact relationship between the two quantities and demonstrate how they depend on the same dynamical correlation functions.

The connection between electron-transfer rates and optical lineshapes may be understood as follows: Reaction rates may be calculated by starting with a nonadiabatic (two-state) model and expanding the rate perturbatively in the nonadiabatic coupling V. Optical lineshapes are usually calculated by expanding the optical polarization in powers of the electric field E. Both expansions are expressed in terms of correlation functions. To lowest order (V^2), the nonadiabatic rate is given by the Fermi golden rule; the optical response to first order in E (e.g., the absorption lineshape) is given by the linear susceptibility $\chi^{(1)}$. Both quantities are related to a two-time correlation function of the solvent. In the next order (V^4), the rate is related to a four-point correlation function. The same correlation function enters in the calculation of the third order nonlinear susceptibility (to order E^3), $\chi^{(3)}$. Numerous nonlinear optical measurements can be interpreted in terms of $\chi^{(3)}$. Fluorescence, coherent and spontaneous Raman, hole-burning, pump-probe, and four wave mixing are a few examples of optical measurements related to $\chi^{(3)}$. The expansions can be carried out to higher orders and, in general, the rate to order V^{2n} is related to $\chi^{(2n-1)}$. This connection establishes a fundamental link between the dynamics of rate processes and nonlinear optical measurements.

Åkesson, et al.,[4] have recently performed electron-transfer experiments on Betaine-30, which is frequently used as a probe of solvent polarity. They find a significant contribution of both solute and solvent modes to the electron-transfer rate. In modelling their experiments, they find that a model proposed by Jortner and Bixon,[7] which explicitly includes solute vibrations in a quantum mechanical fashion, does rather well at predicting the electron-transfer rate for solvents such as acetone which have fast relaxation timescales (~ 1 ps). However, for more slowly relaxing solvents, such as triacetin (relaxation timescales ~ 100 ps - 10 ns, depending on temperature), that theory gives reaction rates which are orders of magnitude too slow. This suggests that when the solvent timescale is very slow it may become irrelevant to the electron-transfer, and some other nuclear relaxation time (e.g. that of a low frequency intramolecular vibration) may take over. The present theory, which incorporates both solvent and intramolecular relaxation, shows this crossover very clearly. Furthermore, we suggest that the solute and solvent dynamics observed in these experiments can be understood in the same way as those which are probed directly in nonlinear optical experiments, such as hole-burning spectroscopy.

II. Response Functions in Nonlinear Optical Spectroscopy and Electron-Transfer

Consider a solute-solvent system with two relevant electronic states, |A> and |B>. |A> and |B> can represent the ground and excited electronic states in an optical experiment, or the initial and final states in an electron-transfer experiment. In addition, there is a coupling between the states. We may write the Hamiltonian for this system as

$$H = |A\rangle H_A\langle A| + |B\rangle (H_B + \hbar\omega_{BA})\langle B| + V(|A\rangle\langle B| + |B\rangle\langle A|) \quad . \tag{1}$$

H_A is the nuclear Hamiltonian while the system is in the |A> state, and H_B is the nuclear Hamiltonian for state |B>. $\hbar\omega_{BA}$ is the difference in ground-state energies between the two states. For an optical experiment, V is equal to $\underset{\sim}{\mu}\cdot\underset{\sim}{E}$, where $\underset{\sim}{\mu}$ is the transition dipole moment between the electronic states and $\underset{\sim}{E}$ is the applied electric field. In an electron-transfer experiment, V is the nonadiabatic coupling between the initial and final states.

In an electron-transfer experiment, the quantity of interest is the rate, K; in an optical measurement, the experimental signal may generally be expressed in terms of the polarization of the system. Both of these quantities may be expressed as perturbation series in the interstate coupling:[8]

$$K = V^2C_2 + V^4C_4 \ \ldots \tag{2a}$$

$$P(\underset{\sim}{r},t) = P^{(1)}(\underset{\sim}{r},t) + P^{(3)}(\underset{\sim}{r},t) + \ldots \tag{2b}$$

For typical experiments on isotropic condensed-phase systems, the odd-order terms in Eq. (2a) vanish, as do the even-order terms in Eq. (2b). We shall focus on the two lowest order nonvanishing terms in each series. For the optical experiments, these are:[8]

$$P^{(1)}(\underset{\sim}{r},t) = -\,2\,|\mu|^2\,\mathrm{Im}\int_0^\infty dt_1\, J(t_1)\, E(\underset{\sim}{r},t-t_1)\,. \tag{3a}$$

and

$$P^{(3)}(\underset{\sim}{r},t) = 2\,|\mu|^4\,\mathrm{Im}\int_0^\infty dt_1\int_0^\infty dt_2\int_0^\infty dt_3$$

$$R(t_3,t_2,t_1)\,E(\underset{\sim}{r},t-t_1-t_2-t_3)\,E(\underset{\sim}{r},t-t_2-t_3)\,E(\underset{\sim}{r},t-t_3)\quad . \tag{3b}$$

Here $J(t_1)$ and $R(t_3, t_2, t_1)$ are the linear and third-order nonlinear response functions, respectively. Im (Re) denotes the imaginary (real) part. $P^{(1)}$ is used to calculate linear optical properties, such as the absorption lineshape. $P^{(3)}$ is relevant to a variety of nonlinear optical experiments, such as hole-burning, coherent and spontaneous Raman spectroscopies, and photon echo. For the case of electron-transfer experiments, the two lowest-order terms in Eq. (2a) are given by:[8]

$$C_2 = 2\,\mathrm{Re}\int_0^\infty dt_1\,J(t_1)\quad , \tag{4a}$$

$$C_4 = 2\,\mathrm{Re}\int_0^\infty dt_1\int_0^\infty dt_2\int_0^\infty dt_3\;[R(t_3,t_2,t_1) - R(t_3,t_2=\infty,t_1)]\quad . \tag{4b}$$

In the limit of weak coupling between the initial and final states of the electron-transfer process, the reaction is in the nonadiabatic limit, and the rate is simply given by V^2C_2. This expression for the rate can be derived using the Fermi golden rule, and the electron-transfer process is then analogous to ordinary (linear) absorption. In general, however, we need all orders in V to adequately calculate the rate. To that end, we approximately resum the series in Eq. (2a) with a Padé approximant:[8]

$$K = \frac{V^2C_2}{1 + V^2(C_4/C_2)}\quad . \tag{5}$$

In the nonadiabatic limit, the electron-transfer rate is given by $K_{NA} = V^2C_2$. In the other extreme (the adiabatic limit), we have $K_{AD} = 1 / \langle\tau\rangle$, where $\langle\tau\rangle = C_4 / (C_2)^2$ is the relaxation timescale (solvent or intramolecular) which controls the adiabatic rate.

Eqs. (3) and (4) show the fundamental connection between electron-transfer and optical experiments: Each observable is related to the linear and nonlinear response functions

$J(t_1)$ and $R(t_3, t_2, t_1)$. While the specific states |A> and |B> may be different for the two types of experiments, we shall show in the following that the relevant response functions can be calculated in the same manner.

III. A Multimode Brownian Oscillator Model for Hole-Burning Spectroscopy

In order to directly compare the experimental observables for electron-transfer and optical experiments, we should focus on a specific four wave mixing technique. To that end, we present formulas for the ordinary (linear) absorption lineshape, and for the pump-probe difference absorption spectrum, for a direct comparison to C_2 and C_4. In a pump-probe absorption experiment, the system is subjected to a pump pulse, centered at time $t=-\tau$, and a probe pulse, centered at $t=0$. The applied electric field is:

$$E(\underset{\sim}{r},t) = E_p(t+\tau)e^{i\,\Omega_p t + i\,\underset{\sim}{k}_P\cdot\underset{\sim}{r}} + E_T(t)e^{i\Omega_T t + i\underset{\sim}{k}_T\cdot\underset{\sim}{r}} + \text{c.c.} \tag{6}$$

Here $E_p(t)$ and $E_T(t)$ are the envelopes of the pump and probe pulses, with center frequencies Ω_P and Ω_T, respectively. The transmitted probe pulse is then frequency-dispersed through a monochromator, and subtracted from the transmitted probe in the absence of the pump pulse. The resulting difference absorption signal, measured at frequency ω_T, is given by:[9]

$$S(\Omega_p, \Omega_T; \omega_T, \tau) = -2\ \mathrm{Im}\ E_T^*(\omega_T)\int_{-\infty}^{\infty} dt\ \exp[i(\omega_T-\Omega_T)t]\ P^{(3)}(\underset{\sim}{k}_T, t) \quad . \tag{7}$$

We now consider a specific model for a solute-solute system which can be applied to both nonlinear optics and electron-transfer. The solute may have several harmonic coordinates, representing the intramolecular vibrations which are strongly coupled to the electronic system. For each mode, the equilibrium position of the oscillator representing the nuclear dynamics of the |A> state is displaced from that of the |B> state. We follow the convention that |a> and |c> represent vibronic eigenstates of the |A> state, and |b> and |d> correspond to levels in the |B> electronic state (Fig. 1).

For the solvent, we use a single Brownian oscillator mode in the overdamped limit.[9] Representing the solvation coordinate by $U \equiv H_B - H_A$,[8] we can express the solvent

contribution to the response functions $J(t_1)$ and $R(t_3, t_2, t_1)$ by the first two moments of U and its two-time correlation function. We define:

$$\lambda \equiv \langle U \rangle \tag{8}$$

$$\Delta^2 \equiv \langle U^2 \rangle - \langle U \rangle^2 \tag{9}$$

and

$$M(t) \equiv \frac{1}{\Delta^2} \mathrm{Re}\left[\langle U(t)\, U \rangle - \langle U \rangle^2\right]$$
$$= e^{-\Lambda t} \quad . \tag{10}$$

For a Debye solvent, Λ^{-1} is the longitudinal relaxation time. This solute-solvent system, for a single solute mode, is illustrated schematically in Figure 1:

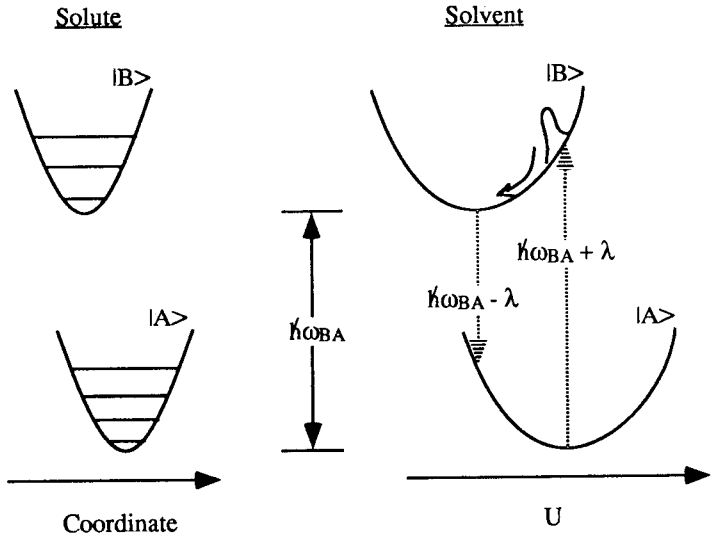

Figure 1: Two-Mode Model for Hole-Burning Spectroscopy

For the solute-solvent system described above, the frequency-dispersed linear absorption is given by:

$$\sigma(\omega_T) = J'(\omega_T - \omega_{BA}) \tag{11}$$

where

$$J'(\omega) = 2\mathrm{Re}\sum_{a,b} P(a)\,|f_{ba}|^2 \int_0^\infty dt_1 \exp\left[\, i(\omega_0 - \omega_{ba})t_1 - g(t_1)\,\right] \tag{12}$$

$$g(t) = i\lambda\int_0^t dt' M(t') + \Delta^2\int_0^t dt'\int_0^{t'} dt'' M(t'') \tag{13}$$

In Eq. (12), f_{ba} represents the Franck-Condon overlap between vibronic states $|b\rangle$ and $|a\rangle$. P(a) is the probability for the solute to be in state $|a\rangle$ at thermal equilibrium.

If we take the solvent nuclear motions to be slow compared with the electronic dephasing timescale, we may perform the integral in Eq. (12), to obtain:[9]

$$J'(\omega) = \sqrt{\frac{2\pi}{\Delta^2}}\sum_{a,b} |f_{ba}|^2 \exp\left[-\frac{1}{2\Delta^2}(\omega - \omega_{ba} - \lambda)^2\right] \tag{14}$$

We next consider an ideal pump-probe experiment in the hole-burning limit, where the pump pulse is long compared to the timescale of the electronic dephasing processes and the pump and probe pulses are well-separated in time. Additionally, we take the probe pulse to be a δ-function in time; since the frequency resolution of the experiment is determined by the monochromator, rather than the probe pulse, this ideal limit does not cause any difficulties. Under these conditions, and further invoking the rotating-wave approximation, the probe difference absorption is given by:

$$S(\Omega_p;\, \omega_T,\, \tau) = |\mu|^4 \int_0^\infty dt_2\; I_P(\tau - t_2)\,[R'(\omega_T - \omega_{BA},\, t_2,\, \Omega_P - \omega_{BA}) + R'(\omega_T - \omega_{BA},\, t_2,\, \omega_{BA} - \Omega_P)] \tag{15}$$

Here $I_P(t)$ is the pump pulse temporal intensity profile, and

$$R'(\omega_3, t_2, \omega_1) = 2\,\mathrm{Re}\int_0^\infty dt_1 \int_0^\infty dt_3\ \exp\left[i\omega_3 t_3 + i\omega_1 t_1\right] R(t_3, t_2, t_1) \tag{16}$$

For the present model, we have[10]

$$R'(\omega_3, t_2, \omega_1) = 2\mathrm{Re}\,|\mu^{(B)}|^4 \int_0^\infty dt_1 \int_0^\infty dt_3 \sum_{a,b,c,d} P(a)\, f_{ab} f_{bc} f_{cd} f_{da} \exp\left[i\omega_3 t_3 + i\omega_1 t_1\right]$$

$$\times \{\exp\left[- i\omega_{dc} t_3 - i\omega_{db} t_2 - i\omega_{da} t_1 - g^*(t_3) - g(t_1) - (z^* - zM(t_1))\, M(t_2)\,(1 - M(t_3))\right]$$

$$+ \exp\left[- i\omega_{dc} t_3 - i\omega_{db} t_2 - i\omega_{da} t_1 - g^*(t_3) - g^*(t_1) - (z - z^* M(t_1))\, M(t_2)\,(1 - M(t_3))\right]$$

$$+ \exp\left[- i\omega_{dc} t_3 - i\omega_{ac} t_2 + i\omega_{ba} t_1 - g(t_3) - g^*(t_1) - z^*(1 - M(t_1))\, M(t_2)\,(1 - M(t_3))\right]$$

$$+ \exp\left[- i\omega_{ba} t_3 - i\omega_{ca} t_2 - i\omega_{da} t_1 - g(t_3) - g(t_1) - z(1 - M(t_1))\, M(t_2)\,(1 - M(t_3))\right] \}\ . \tag{17}$$

Here

$$z = \frac{\Lambda^2}{\Lambda^2} - \frac{2\lambda}{\Lambda}\ .$$

The third - order response function for the system, given by the integrand in eq. (17) is the result of considering the system's dynamics in the following way: Initially, the system is in thermal equilibrium, with electronic density matrix $\rho = |A><A|$. The system then interacts with the pump pulse, leaving ρ in an electronic coherence (either $|A><B|$ or $|B><A|$), where it evolves for a time period t_1. The system then interacts again with the pump pulse, bringing the system back to an electronic coherence (note, however, that the system may then be in a vibrational coherence, e.g. $|b><d|$), where it evolves for a period t_2. The first two terms in eq. (17) correspond to the system propagating on the $|B>$ electronic state during t_2, while the last two terms involve propagation in the $|A>$ state. The system then interacts with the probe pulse, after which it evolves in an electronic coherence during the time period t_3. Following that time period, the detection of the signal takes place. It should be noted that in the current model we have chosen to represent the solute modes using the vibronic state

representation. Alternatively, we can use the Wigner phase space representation to model the solute modes[9]; the choice of representation is made for convenience of calculation; if the solute modes are low-frequency, the phase space representation may become more convenient.

Assuming the solvent nuclear motions to be slow compared to the timescale of the electronic dephasing, and making the additional assumption that the system evolves in a vibrational population during the t_2 time period (i.e. considering only terms with b = d in the first two terms of Eq. (17) and a = c in the last two terms), we obtain:

$$R'(\omega_3, t_2, \omega_1) = \sum_{a,\,b,\,d} P(a)\,|f_{ab}|^2\,|f_{ad}|^2\,\frac{2\pi}{\Delta^2[1-M^2(t_2)]^{1/2}}$$

$$\times \exp\left\{\frac{1}{\Delta^2 - \Delta^2 M^2(t_2)}\left[-\frac{1}{2}(\omega_3 - \omega_{da} - \lambda)^2 - \frac{1}{2}(\omega_1 - \omega_{ba} - \lambda)^2\right.\right.$$

$$\left.\left. + M(t_2)(\omega_3 - \omega_{da} - \lambda)(\omega_1 - \omega_{ba} - \lambda)\right]\right\}$$

$$+ \sum_{a,\,b,\,c} P(a)\,|f_{ab}|^2\,|f_{cb}|^2\,\frac{2\pi}{\Delta^2[1-M^2(t_2)]^{1/2}}$$

$$\times \exp\left\{\frac{1}{\Delta^2 - \Delta^2 M^2(t_2)}\left[-\frac{1}{2}(\omega_3 - \omega_{bc} - \lambda(t_2))^2 - \frac{1}{2}(\omega_1 - \omega_{ba} - \lambda)^2\right.\right.$$

$$\left.\left. + M(t_2)(\omega_3 - \omega_{bc} - \lambda(t_2))\,(\omega_1 - \omega_{ba} - \lambda)\right]\right\} \qquad (18)$$

with

$$\lambda(t) \equiv \lambda[2M(t) - 1] \quad .$$

The neglect of the vibrational coherence terms (propagation with $b \neq d$ or $a \neq c$ during t_2) may be justified for high frequency vibrations. The fast oscillations during the t_2 period make their contribution small. This is not true for vibrations of lower frequency.

We have calculated the hole-burning spectrum for a two-mode system, with the following parameters: The solute mode has frequency $\omega = 600$ cm^{-1}, and the oscillators are displaced by a dimensionless displacement d = 1.2. The solute mode has $\lambda = 625$ cm^{-1}, $\Delta = 510$ cm^{-1}, and $\Lambda^{-1} = 3.5$ picoseconds. The pump pulse is 62 fs fwhm, and the probe pulse is taken to be a δ-function. Figure 2 illustrates the frequency-resolved hole-burning signal for three delay times: $\tau = 200$ fs, 600 fs, and 8 ps:

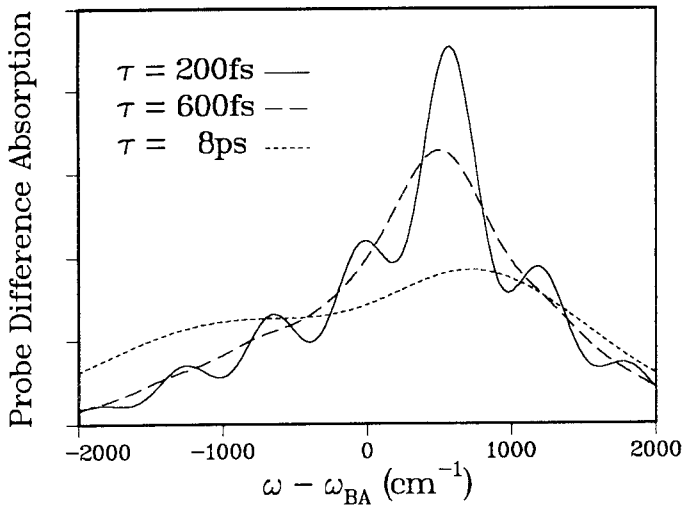

Figure 2: Hole-Burning Spectra for 3 Delay Times.

In the shortest of the delay times, we see peaks due to vibronic transitions in the solute mode. This narrowing results from the spectral selectivity of the initial excitation, whereby the inhomogeneous broadening of the solvent is eliminated, and the underlying vibronic structure is then visible. At longer times, the solvent mode broadens the spectrum, causing the vibronic peaks to be smeared out in the $\tau = 600$ fs curve. At still longer times, the solvent mode causes a Stokes shift in the difference absorption signal, whereby the contributions from excited-state propagation during the t_2 time period are separated from ground-state the ground-state propagation part.[11]

IV. The Multimode Electron-Transfer Rate

For electron-transfer experiments, we may use a model virtually identical to the one described in the previous section, as illustrated in Figure 3:

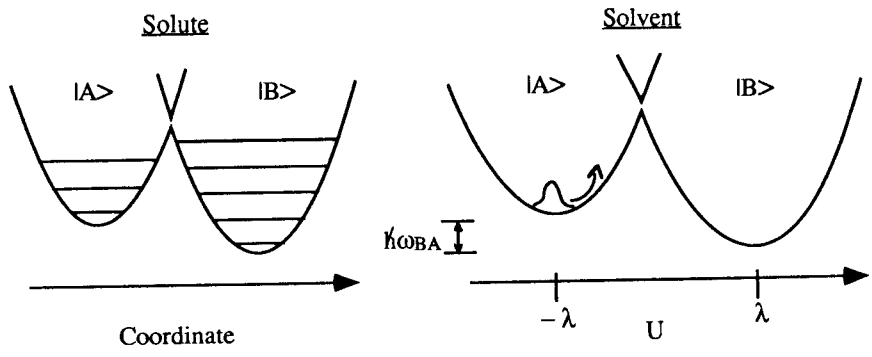

Figure 3: Two-Mode Model for Electron-Transfer

For this solute-solute system, eqs. (4) become[8]

$$C_2 = J'(-\omega_{BA}) \tag{19a}$$

and

$$C_4 = \int_0^\infty dt_2\ [R'(-\omega_{BA}, t_2, -\omega_{BA}) - R'(-\omega_{BA}, t_2 = \infty, -\omega_{BA})]\ , \tag{19b}$$

where J' and R' are given by Eqs. (14) and (17), respectively. Inserting Eqs. (19) into Eq. (5) gives us the electron-transfer rate for the multimode Brownian oscillator model. In general, the parameters used in calculating J' and R' for the two types of experiments could be different, as the two experiments probe different electronic states. However, the physical significance of the parameters are the same, and we can thus consider the two types of experiments using the same theoretical framework. Eq. (19b) allows us to identify the relevant molecular dynamics timescale which controls the adiabatic electron-transfer rate. In many cases, this is due to the solvent relaxation time. However, if that timescale is very slow, other processes (such as the vibrational relaxation of the low frequency modes) may take over and dominate the relaxation of R' to its $t_2 = \infty$ value. Since R' is a multimode quantity which depends on solvent dynamics as well as intramolecular vibrations, Eq. (19b) can be used in either case.

The expression for the electron-transfer rate, given by Eq. (5) is similar, but not identical, to one presented recently by Jortner and Bixon.[7] The main difference is that Jortner and Bixon assume the rate to be the sum of contributions from pairs of vibrational levels in the initial and final state. In resumming eq. (2a) to obtain eq. (5), we could have made the same

assumption. Rather than expressing the electron-transfer rate as the sum of contributions from separate "reaction channels", we have used a different resummation of the perturbation series in V. Furthermore, the analogy with nonlinear optics allows us to explicitly consider the intermediate vibrational states involve in the reaction process, rather than just the initial and final vibrational states. In general, the contributions of the various modes to the rate are nonadditive, just as the various contributions to the hole-burning spectra are not additive. However, if we neglect the contributions of vibrational coherences (i.e. terms with $b \neq d$ and $a \neq c$) to the rate, as we have done here, we could rewrite the series in Eq. (2a) in terms of a sum over reaction channels; thus, a rearrangement of that series, followed by a Padé resummation, would produce a similar result to that of Jortner and Bixon.

In conclusion, we have shown how a unified treatment of nonlinear optics and electron-transfer kinetics may be used to clarify the different solute and solvent contributions to the electron-transfer rate. It is thus, in principle, possible to used the results of nonlinear optical experiments, which probe the specific characters of the solute and solvent modes, to obtain parameters necessary for the calculation of electron-transfer rates.

Acknowledgements

We would like to thank Prof. P. Barbara for useful discussions. The support of the Center for Photoinduced Charge Transfer sponsored by the National Science Foundation, the Air Force Office of Scientific Research, and the Petroleum research fund, administered by the American Chemical Society, is gratefully acknowledged.

References

1. C. H. Brito-Cruz, R. L. Fork, W. H. Knox, and C. V. Shank, Chem. Phys. Lett., **132**, 341 (1986).
2. P. C. Becker, H. L. Fragnito, J. Y. Bigot, C. H. Brito-Cruz, R. L. Fork, and C. V. Shank, Phys. Rev. Lett., **63**, 505 (1989).
3. N. Mataga, Bull. Chem. Soc. Japan, **36**, 654 (1963); N. Mataga, T. Okada, Y. Kanda, and H. Shioyama, Tetrahedron, **42**, 6143 (1986); N. Mataga, Pure and Applied Chemistry, **56**, 1255 (1984); H. Masuhara and N. Mataga, Acc. Chem. Res., **14**, 312 (1981).
4. E. Åkesson, G. C. Walker, and P. F. Barbara, J. Chem. Phys (submitted).

5. M. Maroncelli, J. MacInnis, and G. R. Fleming, Science, **243**, 1674 (1989).
6. J. D. Simon, Acc. Chem. Res., **21**, 128 (1988).
7. J. Jortner and M. Bixon, J. Chem. Phys. **88**, 167 (1988).
8. Y.J. Yan, M, Sparaglione, and S. Mukamel, J. Phys. Chem., **92**, 4842 (1988); S. Mukamel and Y. J. Yan, Acc. Chem. Res., **22**, 301 (1989).
9. Y.J. Yan and S. Mukamel, Phys. Rev. A, **41**, 6485 (1990).
10. S. Mukamel and Y.J. Yan in Recent Trends in Raman Spectroscopy, S. B. Banerjee and S. S. Jha, Eds., World Scientific, Singapore (1989), pp. 160-191.
11. W. B. Bosma, Y.J. Yan, and S. Mukamel, J. Chem. Phys., **93**, 3863 (1990).

DISCUSSION

Fleming

Could you comment on the Non-Markovian interpretation of their recent 3-pulse photon echo experiments by Shank and coworkers?

Mukamel

The three pulse echo experiments cannot be adequately interpreted using the stochastic model. That model neglects completely the effect of the chromophore on the solvent dynamics and therefore misses the Stokes shift which occurs during the t_2 period (delay between the second and the third pulses). The model result may be obtained by setting $\lambda=0$ in eq (13) thereby taking g(t) to be real. The Brownian oscillator model does incorporate the Stokes shift properly. Three pulse echo measurements provide therefore very valuable dynamical information which is not contained in two pulse echoes. Apart from showing the Stokes shift and establishing a connection with fluorescence, three pulse echo measurements can also have a simple Fourier transform relation with hole burning when the delay time t_2 is sufficiently large [Y. J. Yan and S. Mukamel, J. Chem. Phys. **94** *179* (1991)].

Hynes

Is it not true that the oscillator model that you use would predict that, for example, the time dependent fluorescence spectral width is either constant or proportional to the square of what you call M(t) [depending on initial conditions]? If so, this seems to be inconsistent with experimental results from the Fleming group and computer simulations [Carter and Hynes, JPC 1991], where widths narrow with a time dependence more like that of the first power of M(t). Can you comment on this?

Mukamel

This is true if you assume a single solvation coordinate. By corporating several overdamped (solvent and molecular) coordinates with different relaxation times and incorporating vibrational relaxation, the time dependence of the width does not have to satisfy a simple relation with the Stokes shift time scale (R. F. Loning, Y. J. Yan and S. Mukamel, J. Chem. Phys. *87*, 5840 (1987)).

Sumi

In your treatment of the rate constant for electron transfer, you assembled a perturbation series by using the Pade approximation to get a compact formula. In the adiabatic limit for a large electron-transfer matrix element V, your formula approaches a dependence proportional to $1/\tau$, where τ represents the relaxation time of Brownian motions. I solved the same problem in which both fast vibrational and slow Brownian motions take part in the reaction, but by a nonperturbational treatment. I could show rigorously that the rate constant approaches, in the adiabatic limit, to a dependence proportional to a fractional (less than unity) power

of $1/\tau$. This means that the Pade approximation cannot be applied in the adiabatic limit for large V. Therefore, the correspondence between the problem of nonlinear spectroscopy and that of the rate constant you pointed out can be obtained only in the nonadiabatic limit for small V, but fails to hold as V increases.

Mukamel

It is true that we have used an approximate resummation procedure in our solution. However, our simulation can give a fractional dependence on the viscosity. [M. Sparpaglione and S. Mukamel, J. Chem. Phys., 88, 4300 (1988)]. Our τ is a complex function of the viscosity which for large viscosities scales as $1/\eta$ but for intermediate viscosities we do get the fractional power dependence of $\eta^{-\alpha}$.

Jortner

I would like to comment briefly on the Zusman limit alluded by you and by Hynes. From a general formalism he derived the expression $k_{ET}=k_{NA}/H$, where k_{NA} is the nonadiabatic rate while $H=V^2C_4/C_2$ in your notation or $H=(4\pi V^2\tau_L/\hbar E_m)$ (where E_m is the medium reorganization energy) as derived by us for a Debye solvent. This equation incorporates the dissipative properties of the solvent in the frequency factor for the rate. What is significant is that the more general expression $k_{ET}=k_{NA}/(1+H)$, which was derived by several groups, bridges between the nonadiabatic limit and the Zusman limit. This last expression should be confronted with the results of simulations and utilized for the interpretation of experimental data.

Mukamel

Our expression agrees with yours and with Zusman's expression for a Debye solvent. Its main advantage is that it provides a simple generalization to any dielectric function $\varepsilon(\omega)$ as well as an arbitrary number of high frequency molecular vibrations. A 29 mode calculation for hole burning illustrates that point (S. Mukamel, Adv. Chem. Phys. **70** *165* (1988)).

Hynes

I believe that there is some confusion arising in the meaning of "adiabatic" in the discussion between Sumi and Mukamel. In the electronically adiabatic limit (i.e., large enough electronic coupling), the barrier height itself is modified (decreased) by the coupling (I think this is also Sumi's sense of "adiabatic"); I do not think that this is included in Mukamel's development. Further, I believe – as indicated in my talk – the solvent dynamical effects arise from events occurring in the neighborhood of the parabolic barrier top. The formula which Mukamel showed – which also appears in J. Phys. Chem. 90, 3701 (1986) – involving M(t), and also the more general formula connecting ET and nonlinear spectroscopy, can only refer to solvent motion in stable solvent wells, and not on the unstable barrier top of relevance for adiabatic reactions (at least for fast solvents).

Mukamel

Our expression is based on a resummation of a perturbative expression for the rate. C_2 and C_4 contain the dynamics of both wells in the absence of nonadiabatic coupling. The full adiabatic expression will require an extension of the present approach.

Jortner

There are two parameters which specify electron transfer dynamics, the Landau Zenner parameter $\gamma_{LZ}=2v^2/\hbar \mid \vec{F}_1-\vec{F}_2 \mid v$ (where F_1 and F_2 are the slopes of the potential curves at the intersection and v the velocity at this point) and the solvent dynamic parameter $H=4\pi V^2\tau_L/\hbar E_m$ (which was referred by us as the "nonadiabaticity parameter"). The electron transfer rate can be described in the γ_{LZ} and plane so that three limits are realized.
(i) Nonadiabatic limit. Both γ_{LZ} and H are small.
(ii) Solvent dynamic controlled limit. Large H.
(iii) Adiabatic transition-state theory limit. Large γ_{LZ} and moderate H.
When we describe the "transition" between limits (i) and (ii) the now familiar expression $k_{ET}=k_{NA}/(1+H)$ is appropriate, while Hynes focused in his presentation at his conference on limit (iii), Rips and myself have attempted to provide an interpolation formulae between the three limits [I. Rips and J. Jortner in "Perspectives in Photosynthesis" Ed. J. Jortner and B. Pullman, Dochecht Publishing Co. (1989)]

Mukamel

I do not need to reply.